

Affine-Invariant Integrated Rank-Weighted Depth: Definition, Properties and Finite Sample Analysis

Guillaume Staerman, Pavlo Mozharovskyi, Stéphan Cléménçon
 LTCI, Télécom Paris, Institut Polytechnique de Paris
 name.surname@telecom-paris.fr

Abstract

Because it determines a center-outward ordering of observations in \mathbb{R}^d with $d \geq 2$, the concept of statistical depth permits to define quantiles and ranks for multivariate data and use them for various statistical tasks (*e.g.* inference, hypothesis testing). Whereas many depth functions have been proposed *ad-hoc* in the literature since the seminal contribution of [1], not all of them possess the properties desirable to emulate the notion of quantile function for univariate probability distributions. In this paper, we propose an extension of the *integrated rank-weighted* statistical depth (IRW depth in abbreviated form) originally introduced in [2], modified in order to satisfy the property of *affine-invariance*, fulfilling thus all the four key axioms listed in the nomenclature elaborated by [3]. The variant we propose, referred to as the Affine-Invariant IRW depth (AI-IRW in short), involves the covariance/precision matrices of the (supposedly square integrable) d -dimensional random vector X under study, in order to take into account the directions along which X is most variable to assign a depth value to any point $x \in \mathbb{R}^d$. The accuracy of the sampling version of the AI-IRW depth is investigated from a nonasymptotic perspective. Namely, a concentration result for the statistical counterpart of the AI-IRW depth is proved. Beyond the theoretical analysis carried out, applications to anomaly detection are considered and numerical results are displayed, providing strong empirical evidence of the relevance of the depth function we propose here.

1 Introduction

Since its introduction in [1], the concept of statistical depth has become increasingly popular in multivariate data analysis. For a distribution P on \mathbb{R}^d with $d > 1$, by transporting the natural order on the real line to \mathbb{R}^d , a depth function $D(\cdot, P) : \mathbb{R}^d \rightarrow \mathbb{R}_+$ provides a center-outward ordering of points in the support of P and can be straightforwardly used to extend the notions of (signed) rank or order statistics to multivariate data, which find numerous applications in Statistics and Machine Learning (*e.g.* robust inference [4, 5], hypothesis testing [6], novelty/anomaly detection [7, 8]). Numerous definitions have been proposed, as alternatives to the earliest proposal, the *halfspace* depth introduced in [1]: among many others, the simplicial depth (see [9]), the projection depth ([10]), the majority depth ([11]), the Oja depth ([4]), the zonoid depth ([12]), the spatial depth ([13] or [14]) or the Monge-Kantorovich depth (see [15]). In order to compare systematically their merits and drawbacks, [3] have devised an axiomatic nomenclature of statistical depths, listing key properties that should be ideally satisfied by a depth function. Roughly, as depth functions serve to define center-outward orderings, if a distribution P on \mathbb{R}^d has a unique center $\theta \in \mathbb{R}^d$ (*i.e.* a symmetry center in a certain sense), the latter should be the deepest point and the depth should decrease along any fixed ray through it. One also expects that a depth function vanishes at infinity and does not depend on the coordinate system chosen. This latter property is usually formulated as *affine invariance*. A more formal description of these four properties is given in Section 2. Beyond the verification of these properties, the pros and cons of any data depth should be considered with regard to the possible existence of algorithms for exact computation in the case of discrete/sampling distributions. In this respect, the extension of

Tukey's halfspace depth recently introduced in [2] and referred to as the integrated rank-weighted (IRW) depth offers many advantages. Rather than computing, for any point x in \mathbb{R}^d , the minimum of the mass $P(\mathcal{H})$ taken over all closed half-spaces $\mathcal{H} = \{x' \in \mathbb{R}^d : \langle x' - x, u_{\mathcal{H}} \rangle \leq 0\}$ with unit normal vector $u_{\mathcal{H}} \in \mathbb{R}^d$ and containing x , it is proposed to replace the infimum by the integral taken w.r.t. all possible directions $u_{\mathcal{H}}$ uniformly (w.r.t. the uniform distribution on the unit sphere), following in the footsteps of the general *integrated dual depth* approach developed in [16]. For a discrete/empirical distribution, the depth thus constructed admits a weighted average representation and can be easily approximated by means of Monte-Carlo methods in contrast to many other depth functions, whose values are defined as solutions of optimization problems, possibly very complex in high dimension. Beyond these computational aspects, it is shown in [2] that the IRW data depth satisfies several desirable properties, see Theorem 2 therein. Unfortunately, it does not fulfill the *affine invariance* property, as the values taken by the IRW depth may possibly highly depending on the system of coordinates chosen to represent the statistical information available, as shown by an illustrative example in the next section. It is the main purpose of this paper to overcome the lack of affine invariance of the IRW depth by proposing a modified version of it, which consists in the IRW depth of the (supposedly square integrable) random vector X with distribution P under study expressed in an orthogonal coordinate system such that its components are linearly uncorrelated, *i.e.* of the random vector whose components are the principal components of X obtained by eigenvalue decomposition of its covariance matrix Σ (Principal Component Analysis). Under the assumption that Σ is definite positive (otherwise, the methodology promoted should be naturally applied after a dimensionality reduction step *i.e.* applied to an appropriate orthogonal projection of the original random vector X), the *affine-invariant* version of the IRW depth (the AI-IRW depth in abbreviated form) of X is the IRW depth of $\Sigma^{-\top/2}X$, denoting by $\Sigma^{-\top/2}$ the inverse of the transpose of the matrix $\Sigma^{1/2}$, the square root of the symmetric positive definite matrix Σ . In this article, we show that the AI-IRW depth inherits all the properties and computational advantages of the IRW depth and remarkably satisfies the *affine-invariance* property in addition. Because its statistical counterpart based on a sample composed of independent copies of the random variable (r.v.) X is a complex functional of the data, involving the square root of the empirical precision matrix, a finite-sample analysis is carried out here. Precisely, a concentration result for the sampling version of the AI-IRW depth is established. Beyond this theoretical analysis, the relevance of the AI-IRW depth notion is also supported by experimental results, showing its advantages over the IRW depth and other depth proposals standing as natural competitors when applied to various statistical tasks, such as anomaly detection or robust statistical inference.

The article is structured as follows. In Section 2, the concept of data depth is briefly reviewed, together with illustrating examples, the integrated rank-weighted depth in particular, and the axiomatic approach developed by [3]. In Section 3, the AI-IRW depth is introduced, its properties are studied and approximation/estimation issues are discussed at length. The accuracy of the empirical is investigated in Section 4 from a nonasymptotic perspective. Section 5 describes experimental results illustrating empirically the advantages of the AI-IRW depth. Finally, some concluding remarks are collected in Section 6. Additional technical details and numerical results are deferred to the Supplementary Material.

2 Background and Preliminaries

The concept of depth function is motivated by the desire to extend the very useful notions of order and (signed) rank statistics in univariate statistical analysis to multivariate situations by means of depth-induced contours. Indeed, such statistics serve to perform a wide variety of tasks, ranging from robust statistical inference to efficient statistical hypothesis testing for instance. The earliest proposal is the half-space depth developed in [1], whose popularity arises in particular from its strong connection with the notion of distribution function in the univariate context. Indeed, for any probability measure P_1 on \mathbb{R} , constructed as a median-oriented distribution function, the univariate halfspace depth is given by:

$$\forall t \in \mathbb{R}, \quad HD_1(t, P_1) = \min \{P_1([-\infty, t]), P_1([t, +\infty])\}. \quad (1)$$

Considering a multivariate r.v. X with probability distribution P on \mathbb{R}^d with $d > 1$, its halfspace depth at $x \in \mathbb{R}^d$ is then defined as the infimum of the probability mass taken over all possible closed halfspace containing x :

$$HD(x, P) = \inf_{u \in \mathbb{S}^{d-1}} \mathbb{P}(\langle u, X \rangle \leq \langle u, x \rangle), \quad (2)$$

denoting by $\langle \cdot, \cdot \rangle$ and $\|\cdot\|$ the usual Euclidean inner product and norm on \mathbb{R}^d , by $\mathbb{S}^{d-1} = \{z \in \mathbb{R}^d : \|z\| = 1\}$ the unit sphere of \mathbb{R}^d w.r.t. the Euclidean norm. The analysis of the halfspace depth (2), probably because of some of its appealing properties (it is quasi-concave, upper semi-continuous), is undeniably the most documented notion of depth function in the statistical literature. It has been proved to fully characterize discrete/empirical distributions in [17]. Asymptotic guarantees (consistency, asymptotic normality) for its sampling version based on independent copies X_1, \dots, X_n of the generic r.v. X (obtained by replacing P in (2) with the empirical distribution $\hat{P} = (1/n) \sum_{i=1}^n \delta_{X_i}$, where δ_x means the Dirac mass at any point x) are established in e.g. [18, 19, 3]. Multivariate location estimators based on it have been investigated in [20] and it has been shown to possess attractive robustness properties. For instance, the asymptotic breakdown point of the Tukey median, i.e. the barycenter of the deepest locations in the sense of (2), is equal to 1/3 for absolutely continuous centrosymmetric distributions, see [20]. Computational issues have also been extensively studied, see [21], [22], [23] or [24] for instance. However, as recalled in the Introduction section, many other notions of depth have been proposed these last decades, far too numerous to be listed in an exhaustive manner here, refer to [25] for an excellent account of the statistical depth theory. In order to guarantee the 'center-outward ordering' interpretation of a depth function $D(\cdot, P) : \mathbb{R}^d \rightarrow \mathbb{R}_+$ of a probability distribution P on \mathbb{R}^d , four key properties have been listed by [3], see also [26] and [25] for a different formulation of the latter. They are recalled below.

P₁ (AFFINE INVARIANCE) Denoting by P_X the distribution of any r.v. X taking its values in \mathbb{R}^d , we have:

$$\forall x \in \mathbb{R}^d, D(Ax + b, P_{AX+b}) = D(x, P_X), \quad (3)$$

for any d -dimensional r.v. X , any $d \times d$ nonsingular matrix A with real entries and any vector b in \mathbb{R}^d .

P₂ (MAXIMALITY AT CENTER) For any probability distribution P on \mathbb{R}^d that possesses a symmetry center x_P (in a sense to be specified), the depth function $D(\cdot, P)$ takes its maximum value at it:

$$D(x_P, P) = \sup_{x \in \mathbb{R}^d} D(x, P). \quad (4)$$

P₃ (MONOTONICITY RELATIVE TO DEEPEST POINT) For any probability distribution P on \mathbb{R}^d with deepest point x_P , the depth at any point x in \mathbb{R}^d decreases as one moves away from x_P along any ray passing through it:

$$\forall \alpha \in [0, 1], D(x, P) \leq D(x_P + \alpha(x - x_P), P). \quad (5)$$

P₄ (VANISHING AT INFINITY) For any probability distribution P on \mathbb{R}^d , the depth function D vanishes at infinity:

$$D(x, P) \rightarrow 0, \text{ as } \|x\| \rightarrow \infty. \quad (6)$$

Various works have examined which of the properties, among those listed above, that are satisfied by specific notions of depth introduced in the literature, see [3]. Some of them are constructed as an infimum over unit-sphere projections of a univariate non parametric statistic such as the projection depth proposed by [27] or those introduced in [28] or [29]. From a practical perspective, computing these projection-based depths involves the use of tools such as manifold optimization algorithms, facing various numerical difficulties as the dimension d increases, see [30]. In addition, the halfspace depth suffers from two major problems: (i) for each data point, taking the direction achieving the minimum to assign a score to it possibly creates a significant sensitivity to noisy directions (ii) the null score assigned to each new data point outside of the convex hull of the support of the distribution P makes the score of such points indistinguishable. A remedy based on Extreme Value Theory has been proposed in [31], which consists in smoothing the halfspace depth beyond the convex hull of the data. However, this variant relies on rather rigid parametric assumptions, is only approximately affine invariant and confronted with the limitation aforementioned regarding the non-smoothed part of the data. Recently, alternative depth functions have been proposed, obtained by replacing the infimum over all possible directions by an integral, see [16]. In [2], a new data depth, referred to as the Integral Rank-Weighted (IRW) depth, is defined by substituting an integral over the sphere \mathbb{S}^{d-1} for the infimum in (2). Here and throughout, the indicator function of any event \mathcal{E} is denoted by $\mathbb{I}\{\mathcal{E}\}$, the spherical probability measure on \mathbb{S}^{d-1} by ω_{d-1} .

Definition 1. ([2]) *The Integrated Rank-Weighted (IRW) depth, $D_{IRW}(\cdot, P)$ relative to a probability distribution P on \mathbb{R}^d is given by: $\forall x \in \mathbb{R}^d$,*

$$D_{IRW}(x, P) = \int_{\mathbb{S}^{d-1}} HD_1(\langle u, x \rangle, P_u) \omega_{d-1}(du) = \mathbb{E}[HD_1(\langle U, x \rangle, P_U)], \quad (7)$$

where P_u is the pushforward distribution of P defined by the projection $x \in \mathbb{R}^d \mapsto \langle u, x \rangle$ and U is a r.v. uniformly distributed on the hypersphere \mathbb{S}^{d-1} .

As explained at length in [2], the data depth (7) gets its name from the fact that it can be represented as a weighted average of a finite set of normalized center-outward ranks and has many advantages over the original halfspace depth (2). First, by construction it is *robust* to noisy directions and *sensitive* to new data point outside of the convex hull of the training dataset both at the same time, fixing then the two problems mentioned above. Moreover, concerning numerical feasibility, the computation of the IRW depth does not require to implement any manifold optimization algorithm and can be approximately made by means of basic Monte Carlo techniques, providing in addition confidence intervals as a by-product, see Remark 1 below. Its contours $\{D_{IRW}(x, P) = \alpha, \alpha \in [0, 1]\}$, also exhibits a higher degree of smoothness in general (the depth function (7) is continuous at any point $x \in \mathbb{R}^d$ that is not an atom for P , cf. Proposition 1 in [2]) and properties \mathbf{P}_2 , \mathbf{P}_3 and \mathbf{P}_4 have been proved to be satisfied by (7), see Theorem 2 in [2].

Remark 1. (MONTE CARLO APPROXIMATION) *Recall that a r.v. uniformly distributed on the hypersphere \mathbb{S}^{d-1} can be generated from a d -dimensional centered Gaussian random vector W with the identity \mathcal{I}_d as covariance matrix: if $W \sim \mathcal{N}_d(0, \mathcal{I}_d)$, then $W/\|W\| \sim \omega_{d-1}$, see [32]. Hence, a basic Monte-Carlo method to approximate (7) would consist in generating $m \geq 1$ independent realizations W_1, \dots, W_m of $\mathcal{N}_d(0, \mathcal{I}_d)$ and compute*

$$\frac{1}{m} \sum_{j=1}^m HD_1(\langle W_j/\|W_j\|, x \rangle, P_{W_j/\|W_j\|}), \quad (8)$$

refer to e.g. [33] for an account of Monte Carlo integration methods.

However, as illustrated by the example below (see also Section D in the Supplementary Material), it does not satisfy the key property \mathbf{P}_1 (affine-invariance) in general. The fact that it is affected by non-uniform scaling is problematic in practice (regarding its interpretability in particular or its use for anomaly detection tasks for instance, see Section 5) and is the main flaw of this approach, as pointed out in [16, 2].

Example 1. *Consider the discrete probability measure P assigning the weight $1/3$ to the bivariate points in $\mathcal{D}_3 = \{(-1, 2), (3, 3), (2, 1)\}$ and let us compute the IRW depth of $x = (0, 1)$ and $y = (3, 2)$ relative to P . It is easy to see that the mappings $u \in \mathbb{S}^1 \mapsto HD_1(\langle u, x \rangle, P_u)$ and $u \in \mathbb{S}^1 \mapsto HD_1(\langle u, y \rangle, P_u)$ take only two values, 0 or $1/3$. Identifying \mathbb{S}^1 as $[0, 2\pi[$, the univariate halfspace depth of x relative to P is then null for any $u \in [\pi/4, \pi/2] \cup [5\pi/4, 3\pi/2]$ and equal to $1/3$ if u belongs to the complementary set. In addition, $HD_1(\langle u, y \rangle, P_u)$ is equal to 0 for any $u \in [3\pi/4, \pi] \cup [7\pi/4, 2\pi]$ and equal to $1/3$ on the complementary set. One may easily check that $D_{IRW}(x, P) = D_{IRW}(y, P) = 0.25$ and the same rank would be then assigned to each point by the IRW depth. Now, multiplying all ordinate values by 2, which is an affine transformation, the univariate halfspace depth of $\tilde{x} = (0, 2)$ is now null for all u in $[\pi/8, \pi/2] \cup [9\pi/8, 3\pi/2]$ while it remains equal to $1/3$ on the complementary set of this region. The depth of \tilde{x} is thus lower than 0.25. On the other hand, the univariate depth of $\tilde{y} = (3, 4)$ is now null on $[7\pi/8, \pi] \cup [15\pi/8, 2\pi]$ while it remains equal to $1/3$ on the complementary set of this interval. It follows that $D_{IRW}(\tilde{x}) = \frac{5}{24} < 0.25 < \frac{7}{24} = D_{IRW}(\tilde{y})$.*

In the next section, we propose a modification of (7), so as to guarantee that the affine-invariance property is always fulfilled, while preserving all the other advantages.

3 Affine-Invariant IRW Depth - Definition and Properties

Here we propose to modify the depth function (7) in order to ensure that property \mathbf{P}_1 is always satisfied when the random vector X with distribution P under study is assumed to be square integrable

with positive definite variance-covariance matrix Σ . Precisely, rather than taking the expectation w.r.t. a random direction U uniformly distributed on \mathbb{S}^{d-1} (i.e. integrating over all possible directions $u \in \mathbb{S}^{d-1}$), one considers the random projections defined by the eigenfunctions of the matrix Σ , i.e. the principal components of the r.v. X . In other words, the expectation is taken w.r.t. the distribution of the random vector $V = \Sigma^{-\top/2}U/||\Sigma^{-\top/2}U||$ valued in \mathbb{S}^{d-1} , yielding the definition below.

Definition 2. (AFFINE-INVARIANT IRW DEPTH) *The Affine-Invariant Integrated Rank-Weighted (AI-IRW) depth, $D_{\text{AI-IRW}}(\cdot, P)$ relative to a square integrable random vector X with probability distribution P on \mathbb{R}^d and positive definite variance-covariance matrix Σ is given by: $\forall x \in \mathbb{R}^d$,*

$$D_{\text{AI-IRW}}(x, P) = \mathbb{E} [HD_1(\langle V, x \rangle, P_V)], \quad (9)$$

where $V = \Sigma^{-\top/2}U/||\Sigma^{-\top/2}U||$ and U being uniformly distributed on the hypersphere \mathbb{S}^{d-1} .

Of course, in the case where the variance-covariance matrix Σ of the supposedly square integrable r.v. X is not invertible, the AI-IRW depth notion should be applied to an orthogonal projection, after an appropriate dimensionality reduction step. As revealed by the proposition stated below, the depth function (9) inherits all the properties of (7) and is remarkably invariant under any affine transformation in addition.

Proposition 1. *The assertions below hold true for any probability distribution P of a square integrable r.v. X valued in \mathbb{R}^d with positive definite variance-covariance matrix.*

- (i) *The AI-IRW depth satisfies the properties $\mathbf{P}_1, \mathbf{P}_2, \mathbf{P}_3$ and \mathbf{P}_4 .*
- (ii) *The AI-IRW depth function is continuous at each point x that is not an atom for P .*

The proof is given in the Supplementary Material. From a computational perspective, The AI-IRW depth can be approximated by Monte Carlo methods in the same way as (7), see Remark 1.

In practice, the distribution P is generally unknown as well as the variance-covariance matrix Σ and only a sample $\mathcal{D}_n = \{X_1, \dots, X_n\}$ composed of $n \geq 1$ independent realizations of the distribution P is available. A statistical counterpart of the AI-IRW depth can be obtained by replacing P with the empirical measure $\hat{P} = (1/n) \sum_{i=1}^n \delta_{X_i}$ and $\Sigma^{-\top/2}$ with an estimator $\hat{\Sigma}^{-\top/2}$ based on \mathcal{D}_n and plugging them next into formula (9) when $\hat{\Sigma}$ is invertible, yielding: $\forall x \in \mathbb{R}^d$,

$$\hat{D}_{\text{AI-IRW}}(x) = \mathbb{E} \left[HD_1(\langle \hat{V}, x \rangle, \hat{P}_{\hat{V}}) \mid \mathcal{D}_n \right], \quad (10)$$

where $\hat{V} = \hat{\Sigma}^{-\top/2}U/||\hat{\Sigma}^{-\top/2}U||$ and U is a r.v. uniformly distributed on \mathbb{S}^{d-1} independent from the X_i 's. From a practical perspective, the (conditional) expectation (10) can also be approximated by means of a basic Monte Carlo scheme, generating a number $m \geq 1$ i.i.d. random directions U_1, \dots, U_m , copies of the generic r.v. U and independent from the original data \mathcal{D}_n : $\forall x \in \mathbb{R}^d$,

$$\tilde{D}_{\text{AI-IRW}}^{\text{MC}}(x) = \frac{1}{m} \sum_{j=1}^m \min \left\{ \hat{F}_{\hat{V}_j}(\langle \hat{V}_j, x \rangle), 1 - \hat{F}_{\hat{V}_j}(\langle \hat{V}_j, x \rangle) \right\}, \quad (11)$$

where, for all $j \in \{1, \dots, m\}$ and $t \in \mathbb{R}$, we set

$$\hat{V}_j = \hat{\Sigma}^{-\top/2}U_j/||\hat{\Sigma}^{-\top/2}U_j|| \text{ and } \hat{F}_{\hat{V}_j}(t) = \frac{1}{n} \sum_{i=1}^n \mathbb{I}_{\{\langle \hat{V}_j, X_i \rangle \leq t\}},$$

with $\mathbb{I}_{\mathcal{E}}$ meaning the indicator function of any event \mathcal{E} . Putting aside the issue of estimating $\Sigma^{-\top/2}$ (discussed below), attention should be paid to the fact that the approximate sample version (11) is very easy to compute (refer to the Section C of the Supplementary Material for further details) and involves no optimization procedure, in contrast to many other notions of depth function.

On estimating the square root of the precision matrix. The simplest way of building an estimate $\hat{\Sigma}^{-\top/2}$ consists in computing the empirical version of the covariance-variance matrix $\hat{\Sigma} = (1/n)XX^\top$, which is a natural and nearly unbiased estimator, and inverting next its square root,

when the latter is positive definite (which happens with overwhelming probability, as shown by the technical analysis carried out in the Supplementary Material). For simplicity, this is the estimation we consider in the finite-sample study presented in the next section. However, alternative techniques can be used, yielding possibly more efficient estimators (under specific assumptions, in high-dimension especially). Shrinkage procedures for covariance estimation under sparsity conditions have been investigated in *e.g.* [34, 35, 36], while a lasso method for direct estimation of the precision matrix, avoiding matrix inversion, is proposed in [37]. Robust covariance estimation techniques, tailored to situations where the data are possibly contaminated or heavy-tailed, have also been documented in the literature, see *e.g.* [38] and [39]. Classically, from a symmetric definite positive estimator of the variance-covariance matrix, one can easily build an estimator of the square root of the precision matrix by inverting a triangular/diagonal matrix. Due to the presence of $\widehat{\Sigma}^{-\top/2}$ in (10) (respectively, in (11)), it is far from straightforward to assess the accuracy of the estimators of the AI-IRW depth proposed above. It is the purpose of the next section to study the uniform deviations between (9) and its empirical versions from a nonasymptotic perspective.

4 Finite-Sample Analysis - Concentration Bounds

We now investigate the accuracy of the statistical version, as well as that of its Monte Carlo approximation, of the AI-IRW depth function introduced in the previous section in a nonasymptotic fashion. Precisely, we establish a non-asymptotic concentration bound for the maximal deviations between the true and estimated AI-IRW depth functions. We assume here that the estimator of the square root of the precision matrix is given by the inverse of the square root of the empirical covariance, when the latter is definite positive (which happens with overwhelming probability), and by that of any definite positive regularized version (*e.g.* Tikhonov) of the latter. The subsequent analysis requires additional hypotheses, listed below. The first assumption stipulates that the eigenvalues $\sigma_1, \dots, \sigma_d$ of the variance-covariance matrix Σ of the square integrable random vectors X considered are bounded away from zero.

Assumption 1. *There exists $\varepsilon > 0$ such that: $\forall j \in \{1, \dots, d\}, \varepsilon \leq \sigma_j$.*

The other assumptions correspond to smoothness conditions of Lipschitz type for the function $\phi : (u, x) \in \mathbb{S}^{d-1} \times \mathbb{R} \mapsto \mathbb{P}\{\langle u, X \rangle \leq \langle u, x \rangle\}$.

Assumption 2. (UNIFORM LIPSCHITZ CONDITION IN PROJECTION) *For all $(x, y) \in \mathbb{R}^d \times \mathbb{R}^d$, there exists $L_p < +\infty$ such that*

$$\sup_{u \in \mathbb{S}^{d-1}} |\phi(u, x) - \phi(u, y)| \leq L_p \|x - y\|.$$

Assumption 3. (UNIFORM RADIAL LIPSCHITZ CONDITION) *For all $(u, v) \in \mathbb{S}^{d-1} \times \mathbb{S}^{d-1}$, there exists $L_R < +\infty$ such that*

$$\sup_{x \in \mathbb{R}^d} |\phi(u, x) - \phi(v, x)| \leq L_R \|u - v\|.$$

Notice that the same assumptions are involved in the non-asymptotic rate bound analysis carried out for the halfspace depth estimator in [40] and are used to establish limit results related to its approximation in [41]. The Lipschitz conditions are satisfied by a large class of probability distributions, for which Lipschitz constants L_R and L_p can be both explicitly derived. For instance, if the distribution P of X has compact support included in the ball $\mathcal{B}(0, r) = \{x \in \mathbb{R}^d : \|x\| \leq r\}$ (relative to the Euclidean norm $\|\cdot\|$) with $r > 0$ and is absolutely continuous w.r.t. Lebesgue measure with a density bounded by $M > 0$, the uniform Lipschitz conditions are then fulfilled with $L_R = MV_{d,r}$ and $L_p = MV_{d-1,r}$ where $V_{d,r} = \pi^{d/2} r^d / \Gamma(d/2 + 1)$ is the volume of the ball $\mathcal{B}(0, r)$ and $z \geq 0 \mapsto \Gamma(z) = \int_0^\infty t^{z-1} e^{-t} dt$ means the Gamma function, refer to the Supplementary Material for further details (see Lemma 6 and 7 therein) and to [40] for additional examples. The bounds stated in the theorem below reveal the accuracy of the statistical estimates (10) and (11) and highlight their behavior through explicit constants.

Theorem 1. *Suppose that the distribution P of the r.v. X satisfies Assumptions 1, 2 and 3. Let γ be the minimum eigengap of Σ , X 's variance-covariance matrix: $\gamma = \min\{\sigma_{(i)} - \sigma_{(i+1)}, 1 \leq i \leq d\}$, where $\sigma_{(1)} > \dots > \sigma_{(d)}$ are Σ 's eigenvalues sorted by decreasing order of magnitude and $\sigma_{(n+1)} = 0$ by convention. The following assertions hold true.*

(i) For any $\delta \in \left(\max\{\Theta, 12.9^d\} e^{-\frac{n}{2} \min\{\alpha, \alpha^2, \alpha\Delta/8\}}, 1 \right)$, we have with probability at least $1 - \delta$:

$$\sup_{x \in \mathbb{R}^d} \left| \hat{D}_{AI-IRW}(x) - D_{AI-IRW}(x, P) \right| \leq \Delta(L_R, d, \gamma, \varepsilon, \tau) \max_{s=1,2} \left(\frac{d+1+\log(2/\delta)}{n} \right)^{1/s} + \sqrt{\frac{8 \log(\Theta/\delta)}{n}},$$

where $\Delta = 256L_R\tau^2 \max\{1/\xi, 2\sqrt{2d}/\gamma\}$ with $\xi \in (0, \varepsilon)$, $\alpha(\varepsilon, \tau) = (\varepsilon - \xi)/(32\tau^2)$ and $\Theta = 12(2n)^{d+1}/(d+1)!$.

(ii) Let $r > 0$. For any $\delta \in \left(\max\{\Theta, 12.9^d\} e^{-n \min\{\alpha, \alpha^2, \alpha\Delta/8\}}, 1 \right)$, we have with probability at least $1 - \delta$:

$$\sup_{x \in \mathcal{B}_r} \left| \hat{D}_{AI-IRW}^{MC}(x) - D_{AI-IRW}(x, P) \right| \leq \sqrt{\frac{128 \log(3\Theta/2\delta)}{9n}} + \frac{8\Delta}{3} \max_{s=1,2} \left(\frac{d+1+\log(2/\delta)}{n} \right) + \frac{4L_p}{3m} + 2\sqrt{\frac{d \log(3rm) + \log(6/\delta)}{18m}},$$

where the constants Θ, Δ, α and the parameter $\xi \in (0, \varepsilon)$ are the same as those involved in (i).

Due to space limitations, the detailed proof is postponed to the Supplementary Material. The upper confidence bound in assertion (i) is decomposed into two terms. The first term, of order $O(n^{-1/2})$ and sublinearly depending on d , owes its presence to the replacement of $\Sigma^{-1/2}$ by its estimator. Observe also that it explodes as γ or ε vanish. The rate is in line with the covariance matrix estimation literature [42, 43, 44, 45, 46] and is actually optimal with the operator norm (see e.g. [44] for a lower bound for the special class of tapering estimators). Notice finally the presence of the free parameter $\xi \in (0, \varepsilon)$ in the bound: the larger ξ , the smaller the constant Δ and the shorter the range of acceptable confidence levels δ (i.e. the smaller α). The second term, of order $O(\sqrt{\log(n)/n})$ and exhibiting a sublinear dependence in the dimension d , corresponds to the bound that would be obtained if $\Sigma^{-1/2}$ were known (it is then derived by means of the arguments used to study the concentration properties of the empirical halfspace depth, see chapter 26 in [47]).

The upper confidence bound in assertion (ii) differs from that in assertion (i) in two respects. First, the additional terms clearly show the effect of the Monte Carlo approximation, which is negligible when $m \gg n$. Second, the maximal deviation is taken over a compact subset of \mathbb{R}^d .

Remark 2. (RELATED WORK) We point out that nonasymptotic results about the accuracy of sample versions of statistical depths, such as those stated above, are seldom in the literature. To the best of our knowledge, rate bounds have only been derived in the halfspace depth case before. The first result (see [47] chapter 26), where uniform rates of the sample version are provided, uses the fact that the set of halfspaces in \mathbb{R}^d is of finite VC dimension. Recently, this result has been refined under the Assumptions 2 and 3 in [40]. Asymptotic rates of convergence for the Monte Carlo approximation of the halfspace depth, i.e., when the minimum over the unit hypersphere is approximated from a finite number of directions, have been recently established in [41]. In contrast to the finite-sample framework, uniform asymptotic rates have been proved in several settings. Unfortunately, approximating a minimum over the unit sphere \mathbb{S}^{d-1} using a Monte Carlo scheme is not optimal. Indeed when the distribution is assumed to belong to a bounded subset of \mathbb{R}^d with bounded density, the authors obtain slow rates of order $O((\log(m)/m)^{1/(d-1)})$ suffering from the curse of dimensionality. Furthermore, they show that obtaining uniform rates of the halfspace depth approximation is not possible in absence of the bounded density assumption (see second example in Section 4.2 in [41]).

5 Numerical Experiments

The advantages of the novel notion of depth introduced in Section 3 are supported by various experimental results in this part. First, we show that the appealing properties (regarding computa-

tion/approximation) of the IRW depth are preserved by the affine invariant version, by exploring empirically the convergence of the returned ranks as the number of sampled projections increases, as well as the variance of its Monte Carlo approximation. Second, the application of the AI-IRW depth to anomaly detection is considered, illustrating clearly the improvement on the performance attained, compared to the IRW depth. Due to space limitations, additional experiments are provided in the Supplementary Material.

On approximating the AI-IRW depth. The accuracy of Monte Carlo approximation, depending on the number m of random directions uniformly sampled, is evaluated for the empirical versions of the AI-IRW depth, the IRW depth, the halfspace depth and the halfspace mass depth [48]. The latter is based on arbitrary cuttings of one-dimensional spaces and may be interpreted as an interpolation between the halfspace depth and the isolation forest algorithm [49, 50, 51]. A robust estimator of the AI-IRW is also introduced using the well-known Minimum Covariance Determinant (MCD) estimator [38] of the sample variance-covariance matrix. The experiment is based on samples of size $n = 100$ drawn from the spherical Cauchy distribution and from the multivariate standard Gaussian distribution (both standard, so that non affine invariant depths are not disadvantaged) in dimension $d = 10$. The classic Kendall τ distance, given by

$$d_{\tau}(\sigma, \sigma') = \frac{2}{n(n-1)} \sum_{i < j} \mathbb{I}_{\{(\sigma(i) - \sigma(j))(\sigma'(i) - \sigma'(j)) < 0\}},$$

for all permutations σ and σ' of the index set $\{1, \dots, n\}$, is used to measure the deviation between the ranks induced by the true depth and those defined by the Monte Carlo approximation of the sampling version. The averaged Kendall τ 's and their empirical 10 – 90 % quantiles (over 100 runs) are displayed in Figure 1. One observes that the approximate empirical AI-IRW depth is not affected by the covariance estimation step, its behavior is similar to that of the approximate empirical IRW depth for the Gaussian distribution when using both covariance estimators. On the other hand, as expected, only MCD behaves similarly to IRW under the heavy-tailed Cauchy model.

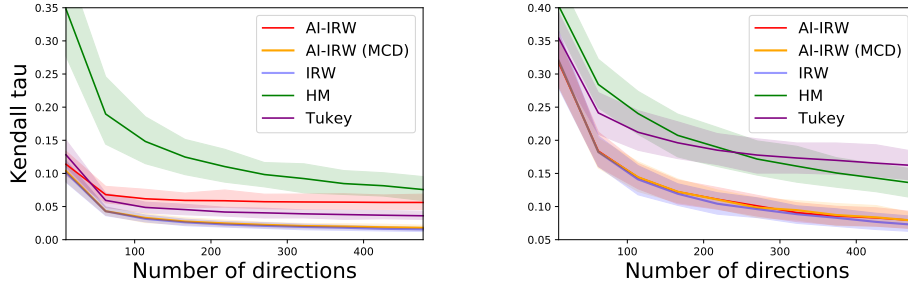


Figure 1: Coherence of the returned rank measured by Kendall τ depending on the number of approximating projections for Cauchy (left) and Gaussian (right) distributions for AI-IRW (using moment and MCD estimates), IRW, halfspace mass (HM) and halfspace (Tukey) depths.

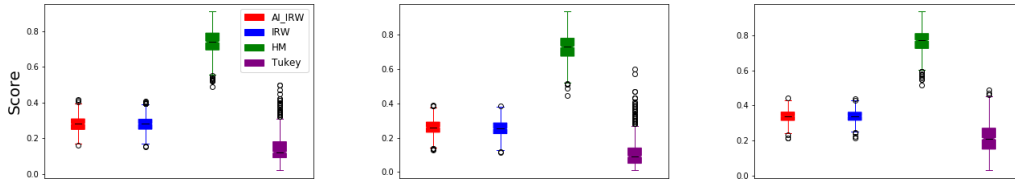


Figure 2: Variance of the score of x_1, x_2, x_3 (from left to right) over 1000 repetitions for the AI-IRW, IRW, halfspace mass (HM) and halfspace (Tukey) depths.

Further, we compare the stability of the approximation estimator AI-IRW measuring its variance. For 100 points stemming from a 10-dimensional Gaussian distribution with zero mean and covariance matrix drawn uniformly on the space of definite matrices, the variance of the returned score is

	n	d	% of anomaly		AI-IRW	IRW	HM	T	IF	AE
Ecoli	195	5	26	Ecoli	0.85	0.83	0.88	0.68	0.77	0.64
Shuttle	49097	9	7	Shuttle	0.99	0.99	0.99	0.86	0.99	0.99
Mulcross	262144	4	10	Mulcross	1	0.98	1	0.87	0.96	1
Thyroid	3772	6	2.5	Thyroid	0.98	0.80	0.84	0.92	0.97	0.97
Wine	129	13	7.7	Wine	0.96	0.96	0.99	0.71	0.8	0.72
Http	567479	3	0.4	Http	1	0.95	0.97	0.99	1	1
Smtip	95156	3	0.03	Smtip	0.96	0.77	0.74	0.85	0.90	0.82
Breastw	683	9	35	Breastw	0.97	0.97	0.99	0.84	0.99	0.91
Musk	3062	166	3.2	Musk	1	0.84	0.97	0.77	1	1
Satimage	5803	36	1.2	Satimage	0.99	0.96	0.98	0.95	0.99	0.98

Table 1: Left: Data sets considered for the performance comparison: n is the number of instances, d is the number of attributes (left). Right: AUROCs of compared anomaly detection methods.

computed on two points close to the center of the distribution (denoted x_1, x_2) and one point in the tail of the distribution (denoted x_3). The score is computed for AI-IRW, IRW, halfspace mass and halfspace depths each approximated using $m = 100$ directions. Figure 2 illustrates that (1) no additional variance is introduced by the affine-invariant version, (2) closeness of the two scores (due to absence of correlation), as well as (3) their higher concentration compared to halfspace mass and halfspace depths.

Application to anomaly detection. To illustrate the performance improvement due to introduction of affine invariance to the IRW, we conduct a comprehensive comparative study of anomaly detection on 10 widely used in the literature data sets¹: *Mulcross*, *Shuttle*, *Thyroid*, *Wine*, *Http*, *Smtip*, *Ecoli*, *Breastw*, *Musk* and *Satimage* varying in size and dimension, see Table 1 (left) for the details. In this unsupervised setting (we train all methods on unlabeled data), we use labels only to assess the performance of the methods by Area Under the Receiver Operation Characteristic curve (AUROC). We contrast the proposed approach with the non affine-invariant version, the original halfspace depth (T), halfspace mass depth (HM), the autoencoder (AE) [52] where the reconstruction error is used as anomaly score and one of the most used multivariate anomaly detection algorithms: isolation forest (IF) [49]. With the performance of these methods being relatively insensitive to their parameters set by default. Since already a moderate number of directions leads to a good approximation of data depth, we adjust it to the data set size setting setting $m = 100 \times d$ for AI-IRW, IRW, halfspace mass and halfspace depths. From Table 1 (right) one observes that AI-IRW uniformly (and significantly in many cases) improves on standard IRW.

6 Conclusion

In this paper, we have introduced a novel notion of statistical depth (AI-IRW), modifying the original Integrated Rank-Weighted (IRW) depth proposal in [2]. The statistical depth we have introduced has been shown not only to inherit all the compelling features of the IRW depth, its theoretical properties and its computational advantages (no optimization problem solving is required to compute it), but also to fulfill in addition the affine invariance property, crucial regarding interpretability/reliability issues. The natural idea at work consists in averaging univariate Tukey halfspace depths computed from random projections of the data onto (nearly) uncorrelated lines, defined by the (empirical) variance-covariance structure of the data, rather than projections onto lines fully generated at random. Though the AI-IRW sample version exhibits a complex probabilistic structure, an estimator of the precision matrix being involved in its definition, a nonasymptotic analysis has been carried out here, revealing its good concentration properties around the true AI-IRW depth. The merits of the AI-IRW depth have been illustrated by encouraging numerical experiments, for anomaly detection purpose in particular, offering the perspective of a widespread use for various statistical learning tasks.

¹<http://odds.cs.stonybrook.edu/>

Acknowledgements

The authors thank Kelly Ramsay for her helpful remarks. This work has been funded by BPI France in the context of the PSPC Project Expresso (2017-2021).

References

- [1] John W. Tukey. Mathematics and the picturing of data. In R.D. James, editor, *Proceedings of the International Congress of Mathematicians*, volume 2, pages 523–531, 1975.
- [2] Kelly Ramsay, Stéphane Durocher, and Alexandre Leblanc. Integrated rank-weighted depth. *Journal of Multivariate Analysis*, 173:51–69, 2019.
- [3] Yijun Zuo and Robert Serfling. General notions of statistical depth function. *The Annals of Statistics*, 28(2):461–482, 2000.
- [4] Hannu Oja. Descriptive statistics for multivariate distributions. *Statistics & Probability Letters*, 1(6):327 – 332, 1983.
- [5] Guillaume Staerman, Pavlo Mozharovskyi, Stéphan Cléménçon, and Florence d’Alché Buc. Depth-based pseudo-metrics between probability distributions, 2021. *ArXiv 2103.12711*.
- [6] Regina Y. Liu and Kesar Singh. Notions of limiting p values based on data depth and bootstrap. *Journal of the American Statistical Association*, 92(437):266–277, 1997.
- [7] Robert Serfling. Depth functions in nonparametric multivariate inference. *DIMACS Series in Discrete Mathematics and Theoretical Computer Science*, 72, 2006.
- [8] Guillaume Staerman, Pavlo Mozharovskyi, and Stéphan Cléménçon. The area of the convex hull of sampled curves: a robust functional statistical depth measure. In *Proceedings of the Twenty Third International Conference on Artificial Intelligence and Statistics*, volume 108, pages 570–579, 2020.
- [9] Regina Y. Liu. On a notion of data depth based upon random simplices. *The Annals of Statistics*, 1990.
- [10] Yijun Zuo. Projection-based depth functions and associated medians. *The Annals of Statistics*, 31(5):1460 – 1490, 2003.
- [11] Regina Y. Liu and Kesar Singh. A quality index based on data depth and multivariate rank tests. *Journal of the American Statistical Association*, 88(421):252–260, 1993.
- [12] Gleb Koshevoy and Karl Mosler. Zonoid trimming for multivariate distributions. *The Annals of Statistics*, 25(5):1998–2017, 10 1997.
- [13] Probal Chaudhuri. On a geometric notion of quantiles for multivariate data. *Journal of the American Statistical Association*, 91(434):862–872, 1996.
- [14] Yehuda Vardi and Cun-Hui Zhang. The multivariate l1-median and associated data depth. *Proceedings of the National Academy of Sciences*, 97(4):1423–1426, 2000.
- [15] Victor Chernozhukov, Alfred Galichon, Marc Hallin, and Marc Henry. Monge–kantorovich depth, quantiles, ranks and signs. *The Annals of Statistics*, 45(1):223–256, 02 2017.
- [16] Antonio Cuevas and Ricardo Fraiman. On depth measures and dual statistics. a methodology for dealing with general data. *Journal of Multivariate Analysis*, 100(4):753–766, 2009.
- [17] Gleb A. Koshevoy. The Tukey depth characterizes the atomic measure. *Journal of Multivariate Analysis*, 83:360–364, 2002.
- [18] Peter J. Rousseeuw and Anja Struyf. Computing location depth and regression depth in higher dimensions. *Statistics and Computing*, 8(3):193–203, 1998.
- [19] David L. Donoho. *Breakdown Properties of Multivariate Location Estimators*. PhD thesis, Harvard University, 1982.
- [20] David L. Donoho and Miriam Gasko. Breakdown properties of location estimates based on halfspace depth and projected outlyingness. *The Annals of Statistics*, 20:1803–1827, 1992.
- [21] Xiaohui Liu and Yijun Zuo. Computing halfspace depth and regression depth. *Communications in Statistics - Simulation and Computation*, 2014.

- [22] Xiaohui Liu. Fast implementation of the Tukey depth. *Computational Statistics*, 32:1395–1410, 2017.
- [23] Xiaohui Liu, Shihua Luo, and Yijun Zuo. Some results on the computing of Tukey’s halfspace median. *Statistical Papers*, 2017. In print. <https://doi.org/10.1007/s00362-017-0941-5>.
- [24] Xiaohui Liu, Karl Mosler, and Pavlo Mozharovskyi. Fast computation of tukey trimmed regions and median in dimension $p > 2$. *Journal of Computational and Graphical Statistics*, 2018. in press.
- [25] Karl. Mosler. Depth statistics. In C. Becker, R. Fried, and S. Kuhnt, editors, *Robustness and Complex Data Structures: Festschrift in Honour of Ursula Gather*, pages 17–34. Springer, 2013.
- [26] Rainer Dyckerhoff. Data depths satisfying the projection property. *AStA - Advances in Statistical Analysis*, 88(2):163–190, 2004.
- [27] Regina Y. Liu. *Data Depth and Multivariate Rank Tests*, page 279–294. 1992.
- [28] Jian Zhang. Some extensions of tukey’s depth function. *Journal of Multivariate Analysis*, 82(1):134–165, 2002.
- [29] Yijun Zuo. Projection-based depth functions and associated medians. *The Annals of Statistics*, 31(5):1460–1490, 2003.
- [30] Rainer Dyckerhoff, Pavlo Mozharovskyi, and Stanislav Nagy. Approximate computation of projection depths, 2020.
- [31] John H.J. Einmahl, Jun Li, and Regina Y. Liu. Bridging centrality and extremity: Refining empirical data depth using extreme value statistics. *The Annals of Statistics*, 43(6):2738–2765, 12 2015.
- [32] Steven G. Krantz and Harold R. Parks. *Geometric Integration Theory*. Birkhäuser, 2008.
- [33] Malvin H. Kalos and Paula A. Whitlock. *Monte Carlo Methods*. Wiley-Blackwell, 2008.
- [34] Olivier Ledoit and Michael Wolf. A well-conditioned estimator for large-dimensional covariance matrices. *Journal of Multivariate Analysis*, 88(2):365–411, 2004.
- [35] Yilun Chen, Ami Wiesel, Yonina C. Eldar, and Alfred O. Hero. Shrinkage algorithms for mmse covariance estimation. *IEEE Transactions on Signal Processing*, 58(10):5016–5029, 2010.
- [36] Juliane Schäfer and Korbinian Strimmer. A shrinkage approach to large-scale covariance matrix estimation and implications for functional genomics. *Statistical applications in genetics and molecular biology*, 4(32), 2005.
- [37] Jerome Friedman, Trevor Hastie, and Robert Tibshirani. Sparse inverse covariance estimation with the graphical lasso. *Biostatistics*, 9(3):432–441, 2008.
- [38] Peter J. Rousseeuw. Least median of squares regression. *Journal of the American Statistical Association*, 79(388):871–880, 1984.
- [39] Peter J. Rousseeuw and Katrien van Driessen. A fast algorithm for the minimum covariance determinant estimator. *Technometrics*, 41(3):212–223, 1999.
- [40] Michael A. Burr and Robert J. Fabrizio. Uniform convergence rates for halfspace depth. *Statistics and Probability Letters*, 124:33 – 40, 2017.
- [41] Stanislav Nagy, Rainer Dyckerhoff, and Pavlo Mozharovskyi. Uniform convergence rates for the approximated halfspace and projection depth. *Electronic Journal of Statistics*, 14(2):3939 – 3975, 2020.
- [42] Joel A. Tropp. User-friendly tail bounds for sums of random matrices. *Foundations of Computational Mathematics*, 12(4):389–434, 2012.
- [43] Joel A. Tropp. An introduction to matrix concentration inequalities. *Foundations and Trends® in Machine Learning*, 8(1-2):1–230, 2015.
- [44] T. Tony Cai, Cun-Hui Zhang, and Harrison H. Zhou. Optimal rates of convergence for covariance matrix estimation. *The Annals of Statistics*, 38(4):2118 – 2144.
- [45] Roman Vershynin. How close is the sample covariance matrix to the actual covariance matrix? *Journal of Theoretical Probability*, 25(3):655–686, 2012.
- [46] T. Tony Cai and Harrison H. Zhou. Optimal rates of convergence for sparse covariance matrix estimation. *The Annals of Statistics*, 40(5):2389 – 2420.

- [47] Galen R. Shorack and Jon A. Wellner. *Empirical Processes with Applications to Statistics*. John Wiley & Sons, 1986.
- [48] Bo Chen, Kai Ming Ting, Takashi Washio, and Gholamreza Haffari. Half-space mass: a maximally robust and efficient data depth method. *Machine Learning*, 100(2):677–699, 2015.
- [49] Fei T. Liu, Kai M. Ting, and Zhi-Hua Zhou. Isolation forest. In *2008 Eighth IEEE International Conference on Data Mining*, 2008.
- [50] S. Hariri, M. Carrasco Kind, and R. J. Brunner. Extended Isolation Forest. *ArXiv e-prints*, 2018.
- [51] Guillaume Staerman, Pavlo Mozharovskyi, Stéphan Cléménçon, and Florence d’Alché Buc. Functional isolation forest. In *Proceedings of The 11th Asian Conference on Machine Learning*, 2019.
- [52] Charu C. Aggarwal. Outlier analysis. *Data Mining*, 2015.
- [53] Per-Åke Wedin. Perturbation theory for pseudo-inverses. *IT Numerical Mathematics*, 1973.
- [54] Roman Vershynin. *High-Dimensional Probability: An Introduction with Applications in Data Science*. Cambridge Series in Statistical and Probabilistic Mathematics. 2018.
- [55] Hermann Weyl. Das asymptotische verteilungsgesetz der eigenwerte linearer partieller differentialgleichungen. *Mathematische Annalen*, 71(4):441–479, 1912.
- [56] Chandler Davis and W. M. Kahan. The rotation of eigenvectors by a perturbation. *SIAM Journal on Numerical Analysis*, 7(1):1–46, 1970.
- [57] Yi Yu, Tengyao Wang, and Richard J. Samworth. A useful variant of the Davis–Kahan theorem for statisticians. *Biometrika*, 102(2):315–323, 2014.

Supplementary Material

This supplementary material is organized as follows:

- Appendix A contains useful preliminary results.
- Appendix B contains the proofs of the porposition and the theorem provided in the paper.
- Appendix C contains the approximation algorithms to compute the AI-IRW depth.
- Appendix D contains additional experiments.

A Preliminary Results

For clarity, this section collects some results on linear algebra, halfspace depth and on sample variance-covariance matrix estimator, used in the subsequent proofs.

A.1 Basics of linear algebra

We now recall useful results in linear algebra.

Lemma 1 ([53], Theorem 4.1). *Let A and B be two invertible matrices of size $d \times d$ and $\|A\|_{op}$ be the operator norm of the matrix A . Then it holds:*

$$\|A^{-1} - B^{-1}\|_{op} \leq \|A^{-1}\|_{op} \|B^{-1}\|_{op} \|A - B\|_{op}. \quad (12)$$

Lemma 2 ([54], lemma 4.4.1). *Let A be a matrix of size $d \times d$ and N_ρ be a ρ -net of \mathbb{S}^{d-1} . Then it holds:*

$$\|A\|_{op} \leq \frac{1}{1 - 2\rho} \max_{v \in N_\rho} |v^\top A v|.$$

Lemma 3. *Let A_1 and A_2 be two real symmetric and invertible matrices of dimension $d \times d$ with $O_1 D_1 O_1^\top$ and $O_2 D_2 O_2^\top$ their eigenvalues decomposition in orthornormal bases. Then it holds:*

$$\|A_1^{-1/2} - A_2^{-1/2}\|_{op} \leq \|D_2^{-1/2}\|_{op} \left(\|D_1^{1/2} - D_2^{1/2}\|_{op} \|D_1^{-1/2}\|_{op} + \|O_1 - O_2\|_{op} \right)$$

Proof.

$$\begin{aligned} \|O_1 D_1^{-1/2} - O_2 D_2^{-1/2}\|_{op} &\leq \|O_1\|_{op} \|D_1^{-1/2} - D_2^{-1/2}\|_{op} + \|O_1 - O_2\|_{op} \|D_2^{-1/2}\|_{op} \\ &\leq \|D_1^{-1/2} - D_2^{-1/2}\|_{op} + \|D_2^{-1/2}\|_{op} \|O_1 - O_2\|_{op} \\ &\stackrel{(5)}{\leq} \|D_2^{-1/2}\|_{op} \left(\|D_1^{1/2} - D_2^{1/2}\|_{op} \|D_1^{-1/2}\|_{op} + \|O_1 - O_2\|_{op} \right), \end{aligned}$$

where (5) holds due to Lemma 1. \square

A.2 Non-asymptotic rates on Halfspace Depth and sample covariance matrix

We now recall results on maximum deviations of the Halfspace depth estimator and on those of the sample variance covariance matrix as well.

Lemma 4 ([47], Chapter 26). *Let $P \in \mathcal{P}(\mathbb{R}^d)$. Let X_1, \dots, X_n a sample from P with empirical measure $\hat{P} = (1/n) \sum_{i=1}^n \delta_{X_i}$. Denote by F_u and \hat{F}_u the cdf of P_u and \hat{P}_u respectively. Then for any $t > 0$ it holds:*

$$\mathbb{P} \left(\sup_{\substack{x \in \mathbb{R}^d \\ u \in \mathbb{S}^{d-1}}} \left| \hat{F}_u(u^\top x) - F_u(u^\top x) \right| > t \right) \leq \frac{6(2n)^{d+1}}{(d+1)!} \exp(-nt^2/8).$$

Lemma 5. Let Σ be the variance-covariance matrix of a τ sub-Gaussian random variables X that takes values in \mathbb{R}^d . Let X_1, \dots, X_n be a sample from X and denote by $\hat{\Sigma} = \frac{1}{n} \sum_{i=1}^n X_i X_i^\top$ the MLE estimator of Σ . Then it holds: $\forall t > 0$,

$$\mathbb{P} \left(\|\hat{\Sigma} - \Sigma\|_{\text{op}} > t \right) \leq 2 \times 9^d \exp \left\{ -\frac{n}{2} \min \left\{ \frac{t^2}{(32\tau^2)^2}, \frac{t}{32\tau^2} \right\} \right\}.$$

Let $\sigma_d > \dots > \sigma_1$ and $\hat{\sigma}_d > \dots > \hat{\sigma}_1$ be respectively the ordered eigenvalues of Σ and $\hat{\Sigma}$. Using Weyl's Theorem [55], it holds:

$$\mathbb{P} \left(\max_{1 \leq i \leq d} |\hat{\sigma}_i - \sigma_i| > t \right) \leq 2 \times 9^d \exp \left\{ -\frac{n}{2} \min \left\{ \frac{t^2}{(32\tau^2)^2}, \frac{t}{32\tau^2} \right\} \right\}.$$

Proof. Let N_ρ be a ρ -net of the sphere \mathbb{S}^{d-1} . Applying Lemma 2 to $\hat{\Sigma} - \Sigma$, for any $t, \rho > 0$, we have

$$\begin{aligned} \mathbb{P} \left(\|\hat{\Sigma} - \Sigma\|_{\text{op}} > t \right) &\leq \mathbb{P} \left(\frac{1}{1-2\rho} \max_{v \in N_\rho} |v^\top (\hat{\Sigma} - \Sigma)v| > t \right) \\ &\leq |N_\rho| \mathbb{P} \left(|v^\top (\hat{\Sigma} - \Sigma)v| > (1-2\rho)t \right), \end{aligned}$$

where $|N_\rho|$ stands for the cardinality of the set N_ρ . Noticing that $\hat{\Sigma} = \frac{1}{n} \sum_{i=1}^n X_i X_i^\top$ is a sum of independent matrices, we have

$$v^\top (\hat{\Sigma} - \Sigma)v = \frac{1}{n} \sum_{i=1}^n Z_i - \mathbb{E}Z_i,$$

where the collection of variables $Z_i = (v^\top X_i)^2$ (respectively, $Z_i - \mathbb{E}Z_i$) are i.i.d and $(16\tau)^2$ sub-exponential (resp., $16\tau^2$) sub-exponential.

Choosing $\rho = 1/4$, noticing that $N_{1/4} \leq 9^d$ and applying the sub-exponential tail bound, one gets the desired result. \square

B Technical Proofs of the Main Results

We now prove the main results stated in the paper.

B.1 Proof of Proposition 1

B.1.1 Affine-Invariance

Let $A \in \mathbb{R}^{d \times d}$ be a non singular matrix and $b \in \mathbb{R}^d$. Let Σ_X and Σ_{AX} the variance-covariance matrix of X and AX respectively. Defines the Cholesky decomposition as $\Sigma_X = \Lambda_X \Lambda_X^\top$ and $\Sigma_{AX} = A \Lambda_X \Lambda_X^\top A^\top = \Lambda_{AX} \Lambda_{AX}^\top$. It holds:

$$\begin{aligned}
D_{\text{AI-IRW}}(Ax + b, AX + b) &= \frac{1}{V_d} \int_{\mathbb{S}^{d-1}} HD_1(\langle \frac{\Lambda_{AX+b}^{-\top} u}{\|\Lambda_{AX+b}^{-\top} u\|}, Ax + b \rangle, \langle \frac{\Lambda_{AX+b}^{-\top} u}{\|\Lambda_{AX+b}^{-\top} u\|}, AX + b \rangle) du \\
&= \frac{1}{V_d} \int_{\mathbb{S}^{d-1}} HD_1(\langle \Lambda_{AX+b}^{-\top} u, Ax + b \rangle, \langle \Lambda_{AX+b}^{-\top} u, AX + b \rangle) du \\
&= \frac{1}{V_d} \int_{\mathbb{S}^{d-1}} HD_1(\langle \Lambda_{AX}^{-\top} u, Ax \rangle, \langle \Lambda_{AX}^{-\top} u, AX \rangle) du \\
&= \frac{1}{V_d} \int_{\mathbb{S}^{d-1}} HD_1(\langle u, \Lambda_X^{-1} x \rangle, \langle u, \Lambda_X^{-1} X \rangle) du \\
&= \frac{1}{V_d} \int_{\mathbb{S}^{d-1}} HD_1(\langle \frac{\Lambda_X^{-\top} u}{\|\Lambda_X^{-\top} u\|}, x \rangle, \langle \frac{\Lambda_X^{-\top} u}{\|\Lambda_X^{-\top} u\|}, X \rangle) du \\
&= D_{\text{AI-IRW}}(x, P).
\end{aligned}$$

The same reasoning applies if the square matrix is given by the SVD decomposition.

B.1.2 Maximality at the Center

Assume that P is halfspace symmetric about a unique β , i.e., $\mathbb{P}(X \in H_\beta) \geq \frac{1}{2}$ for every closed halfspace H_β such that $\beta \in \partial H$ with ∂H the boundary of H . Thus, it is easy to see that $D_{\text{AI-IRW}}(\beta, P) \geq \frac{1}{2}$. The uniqueness of β combined with the fact that $D_{\text{AI-IRW}}$ is lower than $1/2$ at any point in \mathbb{R}^d by definition implies $\beta = \operatorname{argsup}_{x \in \mathbb{R}^d} D_{\text{AI-IRW}}(x, P)$.

B.1.3 Vanishing at Infinity

The proof can be derived from that of Theorem 1 in [16]. We detail it for the sake of clarity. Let U be a random variable following ω_{d-1} , the uniform measure on the unit sphere \mathbb{S}^{d-1} . Defines $V = \Sigma^{-\top/2} U / \|\Sigma^{-\top/2} U\|$ and ν_{d-1} its probability distribution. Let $\theta > 0$, then, $r(\theta) := \nu_{d-1}\{v : \frac{|\langle v, x \rangle|}{\|x\|} \leq \theta\}$ vanishes as $\theta \rightarrow 0$. For any $x \in \mathbb{R}^d \setminus \{0\}$,

$$\begin{aligned}
D_{\text{AI-IRW}}(x, P) &= \int_{\mathbb{R}^d} \min\{F_v(v^\top x), 1 - F_v(v^\top x)\} d\nu_{d-1}(v) \\
&\leq \int_{\mathbb{R}^d} \mathbb{I}\left\{v : \frac{|\langle v, x \rangle|}{\|x\|} \leq \theta\right\} d\nu_{d-1}(v) \\
&+ \int_{\mathbb{R}^d} F_v(v^\top x) \mathbb{I}\left\{v : \frac{|\langle v, x \rangle|}{\|x\|} > \theta, \langle v, x \rangle \leq 0\right\} d\nu_{d-1}(v) \\
&+ \int_{\mathbb{R}^d} (1 - F_v(v^\top x)) \mathbb{I}\left\{v : \frac{|\langle v, x \rangle|}{\|x\|} > \theta, \langle v, x \rangle > 0\right\} d\nu_{d-1}(v) \\
&\leq r(\theta) + \int_{\mathbb{R}^d} F_v(-\varepsilon\|x\|) \mathbb{I}\left\{v : \frac{|\langle v, x \rangle|}{\|x\|} > \varepsilon, \langle v, x \rangle \leq 0\right\} d\nu_{d-1}(v) \\
&+ \int_{\mathbb{R}^d} (1 - F_v(\varepsilon\|x\|)) \mathbb{I}\left\{v : \frac{|\langle v, x \rangle|}{\|x\|} > \varepsilon, \langle v, x \rangle > 0\right\} d\nu_{d-1}(v)
\end{aligned}$$

Now, when $\|x\| \rightarrow \infty$, the dominated convergence theorem ensures that

$$\lim_{\|x\| \rightarrow \infty} \sup D_{\text{AI-IRW}}(x, P) \leq r(\theta) \xrightarrow{\theta \rightarrow 0} 0.$$

B.1.4 Proof of Decreasing along rays

The proof is a slight modification of that of the assertion (iii) in Theorem 2 in [2]. Details are left to the reader.

B.1.5 Continuity

For any $P \in \mathcal{P}(\mathbb{R}^d)$, the continuity of the scalar product and that of the cdf ensures that $HD(v^\top x, v^\top X)$ is continuous for any $v \in \mathbb{S}^{d-1}$. Therefore, the continuity of $x \mapsto D_{\text{AI-IRW}}(x, P)$ follows from dominated convergence theorem.

B.2 Proof of Theorem 1

We now prove the main result of the paper.

B.2.1 Assertion (i)

Introducing terms and using triangle inequality, it holds:

$$\sup_{x \in \mathbb{R}^d} \left| \hat{D}_{\text{AI-IRW}}(x) - D_{\text{AI-IRW}}(x, P) \right| \leq \underbrace{\sup_{x \in \mathbb{R}^d} \left| \hat{F}_{\hat{V}}(\hat{V}^\top x) - F_{\hat{V}}(\hat{V}^\top x) \right|}_{(1)} + \underbrace{\sup_{x \in \mathbb{R}^d} \left| F_{\hat{V}}(\hat{V}^\top x) - F_V(V^\top x) \right|}_{(2)}.$$

Now, the first term (1) can be controlled using the bound for the deviations of Halfspace Depth recalled in Lemma 4. Thus, for any $t > 0$, it holds:

$$\begin{aligned} \mathbb{P} \left(\sup_{x \in \mathbb{R}^d} \left| \hat{F}_{\hat{V}}(\hat{V}^\top x) - F_{\hat{V}}(\hat{V}^\top x) \right| > t/2 \right) &\leq \mathbb{P} \left(\sup_{\substack{y \in \mathbb{R}^d \\ u \in \mathbb{S}^{d-1}}} \left| \hat{F}_u(u^\top y) - F_u(u^\top y) \right| > t/2 \right) \\ &\leq \frac{6(2n)^{d+1}}{(d+1)!} \exp(-nt^2/32). \end{aligned} \quad (13)$$

The second term (2) relies on the influence of the deviations of the sample variance-covariance matrix. First, observe that

$$\begin{aligned} \sup_{x \in \mathbb{R}^d} \left| F_{\hat{V}}(\hat{V}^\top x) - F_V(V^\top x) \right| &\leq \sup_{\substack{x \in \mathbb{R}^d \\ u \in \mathbb{S}^{d-1}}} \left| \mathbb{P} \left(\left\langle \frac{\hat{\Sigma}^{-\top/2} u}{\|\hat{\Sigma}^{-\top/2} u\|}, X - x \right\rangle \leq 0 \mid \mathcal{S}_n \right) \right. \\ &\quad \left. - \mathbb{P} \left(\left\langle \frac{\Sigma^{-\top/2} u}{\|\Sigma^{-\top/2} u\|}, X - x \right\rangle \leq 0 \right) \right|. \end{aligned}$$

Now, since X is radially Lipschitz continuous, we have

$$\left| \mathbb{P} \left(\left\langle \frac{\hat{\Sigma}^{-\top/2} u}{\|\hat{\Sigma}^{-\top/2} u\|}, X - x \right\rangle \leq 0 \mid \mathcal{S}_n \right) - \mathbb{P} \left(\left\langle \frac{\Sigma^{-\top/2} u}{\|\Sigma^{-\top/2} u\|}, X - x \right\rangle \leq 0 \right) \right| \leq L_R \left\| \frac{\hat{\Sigma}^{-\top/2} u}{\|\hat{\Sigma}^{-\top/2} u\|} - \frac{\Sigma^{-\top/2} u}{\|\Sigma^{-\top/2} u\|} \right\|.$$

Introducing terms and using triangle inequality, we can write

$$\begin{aligned} \left\| \frac{\hat{\Sigma}^{-\top/2} u}{\|\hat{\Sigma}^{-\top/2} u\|} - \frac{\Sigma^{-\top/2} u}{\|\Sigma^{-\top/2} u\|} \right\| &\leq \frac{\|\hat{\Sigma}^{-1/2} - \Sigma^{-1/2}\|_{\text{op}}}{\|\Sigma^{-1/2} u\|} + \|\hat{\Sigma}^{-1/2} u\| \left(\frac{1}{\|\hat{\Sigma}^{-1/2} u\|} - \frac{1}{\|\Sigma^{-1/2} u\|} \right) \\ &\leq \frac{2\|\hat{\Sigma}^{-1/2} - \Sigma^{-1/2}\|_{\text{op}}}{\|\Sigma^{-1/2} u\|}, \end{aligned}$$

yielding

$$\sup_{x \in \mathbb{R}^d} \left| F_{\hat{V}}(\hat{V}^\top x) - F_V(V^\top x) \right| \leq \frac{2L_R}{\|\Sigma^{-1/2}\|_{\text{op}}} \|\hat{\Sigma}^{-1/2} - \Sigma^{-1/2}\|_{\text{op}}. \quad (14)$$

Assume that ODO^\top and $\hat{O}\hat{D}\hat{O}^\top$ are the eigenvalues decomposition of Σ and $\hat{\Sigma}$ in orthonormal bases. Thus, thanks to Lemma 3, we have

$$\|\hat{\Sigma}^{-1/2} - \Sigma^{-1/2}\|_{\text{op}} \leq \|\Sigma^{-1/2}\|_{\text{op}} \left(\|\hat{D}^{1/2} - D^{1/2}\|_{\text{op}} \|\hat{D}^{-1/2}\|_{\text{op}} + \|\hat{O} - O\|_{\text{op}} \right).$$

Now, since $\min_{i \leq d} \sqrt{\hat{\sigma}_i} \geq \sqrt{\varepsilon} - \max_{i \leq d} |\sqrt{\hat{\sigma}_i} - \sqrt{\sigma_i}|$ and $\max_{i \leq d} |\sqrt{\hat{\sigma}_i} - \sqrt{\sigma_i}| \leq \frac{1}{\sqrt{\varepsilon}} \max_{1 \leq i \leq d} |\hat{\sigma}_i - \sigma_i|$, using Weyl's inequality leads to

$$\sup_{x \in \mathbb{R}^d} \left| F_{\hat{V}}(\hat{V}^\top x) - F_V(V^\top x) \right| \leq 2L_R \left(\frac{\|\hat{\Sigma} - \Sigma\|_{\text{op}}}{\varepsilon - \|\hat{\Sigma} - \Sigma\|_{\text{op}}} + \|\hat{O} - O\|_{\text{op}} \right).$$

By \mathcal{A}_ξ it is denoted the event $\mathcal{A}_\xi = \left\{ \|\hat{\Sigma} - \Sigma\|_{\text{op}} < \varepsilon - \xi \right\}$ for any $\xi \in [0, \varepsilon)$. Using union bound and combining (14) with the previous equation, for any $t > 0$ and $\xi \in (0, \varepsilon)$ it holds:

$$\begin{aligned} \mathbb{P} \left(\sup_{x \in \mathbb{R}^d} \left| F_{\hat{V}}(\hat{V}^\top x) - F_V(V^\top x) \right| > t/2 \right) &\leq \mathbb{P} \left(\frac{2L_R}{\xi} \|\hat{\Sigma} - \Sigma\|_{\text{op}} > t/4 \right) + \mathbb{P}(\mathcal{A}_\xi^c) \\ &\quad + \mathbb{P} \left(2L_R \|\hat{O} - O\|_{\text{op}} > t/4 \right), \end{aligned}$$

where \mathcal{A}_ξ^c stands for the complementary event of \mathcal{A}_ξ .

Applying Lemma 5 leads to

$$\mathbb{P} \left(\|\hat{\Sigma} - \Sigma\|_{\text{op}} > \frac{\xi t}{8L_R} \right) \leq 2 \times 9^d \exp \left\{ -\frac{n}{2} \min \left\{ \frac{(\xi t)^2}{(256L_R\tau^2)^2}, \frac{\xi t}{256L_R\tau^2} \right\} \right\}, \quad (15)$$

and

$$\mathbb{P}(\mathcal{A}_\xi^c) \leq 2 \times 9^d \exp \left\{ -\frac{n}{2} \min \left\{ \frac{(\varepsilon - \xi)^2}{(32\tau^2)^2}, \frac{\varepsilon - \xi}{32\tau^2} \right\} \right\}. \quad (16)$$

Furthermore, it is easy to see that $\|\hat{O} - O\|_{\text{op}} \leq \sqrt{d} \max_{k \leq d} \|\hat{O}_k - O_k\|$, where O_k is the k -th column of the matrix O . Let γ be the minimum eigengap, using a variant of the Davis-Kahan theorem [56] (see Corollary 1 in [57]), it holds:

$$\|\hat{O} - O\|_{\text{op}} \leq \frac{2\sqrt{2d}\|\hat{\Sigma} - \Sigma\|_{\text{op}}}{\gamma}.$$

Using Lemma 5 again, one obtains:

$$\mathbb{P} \left(\frac{4L_R\sqrt{2d}\|\hat{\Sigma} - \Sigma\|_{\text{op}}}{\gamma} > t/4 \right) \leq 2 \times 9^d \exp \left\{ -\frac{n}{2} \min \left\{ \frac{(\gamma t)^2}{(512L_R\sqrt{2d}\tau^2)^2}, \frac{\gamma t}{512L_R\sqrt{2d}\tau^2} \right\} \right\}. \quad (17)$$

Combining (15), (16) and (17), we get:

$$\mathbb{P} \left(\sup_{x \in \mathbb{R}^d} \left| F_{\hat{V}}(\hat{V}^\top x) - F_V(V^\top x) \right| > t/2 \right) \leq 6 \times 9^d \exp \left(-\frac{n}{2} \min \left\{ (\kappa t)^2, \kappa t \right\} \right),$$

for any $t \leq (\varepsilon - \xi)/(32\tau^2\kappa)$ where $\kappa = \frac{1}{256L_R\tau^2} \left(\xi \wedge \frac{\gamma}{2\sqrt{2d}} \right)$. Finally, for any $t \leq (\varepsilon - \xi)/(32\tau^2\kappa)$ it holds:

$$\mathbb{P} \left(\sup_{x \in \mathbb{R}^d} \left| \hat{D}_{\text{AI-IRW}}(x) - D_{\text{AI-IRW}}(x, P) \right| > t \right) \leq 6.9^d \exp \left(-\frac{n}{2} \min \{ (\kappa t)^2, \kappa t \} \right) + \frac{6(2n)^{d+1}}{(d+1)!} \exp(-nt^2/32), \quad (18)$$

and the desired bound is then easily obtained.

B.2.2 Assertion (ii)

Let \mathcal{B}_r be a centered ball of \mathbb{R}^d with radius $r > 0$ and assume that X satisfies Assumption 2 for any $x \in \mathcal{B}_r$. Introducing terms and using triangle inequality, one gets:

$$\begin{aligned} \sup_{x \in \mathcal{B}_r} \left| \hat{D}_{\text{AI-IRW}}^{\text{MC}}(x) - D_{\text{AI-IRW}}(x, P) \right| &\leq \underbrace{\sup_{x \in \mathbb{R}^d} \left| \hat{D}_{\text{AI-IRW}}(x) - D_{\text{AI-IRW}}(x, P) \right|}_{(1)} \\ &\quad + \underbrace{\sup_{x \in \mathcal{B}_r} \left| D_{\text{AI-IRW}}^{\text{MC}}(x, P) - D_{\text{AI-IRW}}(x, P) \right|}_{(2)}. \end{aligned}$$

The first term (1) can be bounded using Assertion (i) while controlling the approximation term (2) relies on classical chaining arguments. As the function $z \mapsto \min(z, 1 - z)$ is 1-Lipschitz for any $z \in (0, 1)$ and by triangle inequality, for any y in \mathcal{B}_r , we have:

$$\left| D_{\text{AI-IRW}}^{\text{MC}}(y, P) - D_{\text{AI-IRW}}(y, P) \right| \leq \frac{1}{m} \sum_{j=1}^m \left| \mathbb{P} \{ \langle V_j, y \rangle \mid V_j \} - \mathbb{P} \{ \langle V, y \rangle \} \right|.$$

Since it is an average of bounded and i.i.d random variables, combining Hoeffding inequality and the union bound, we have, for any $t > 0$ and any y in \mathcal{B}_r ,

$$\mathbb{P} \left(\left| D_{\text{AI-IRW}}^{\text{MC}}(y, P) - D_{\text{AI-IRW}}(y, P) \right| > t/2 \right) \leq 2 \exp(-nt^2/2). \quad (19)$$

As X is uniformly continuous Lipschitz in projection for any $u \in \mathbb{S}^{d-1}$, observe that, $\forall (x, y) \in \mathcal{B}_r^2$, it holds:

$$\begin{aligned} \left| D_{\text{AI-IRW}}^{\text{MC}}(x, P) - D_{\text{AI-IRW}}(x, P) \right| &\leq \left| D_{\text{AI-IRW}}^{\text{MC}}(x, P) - D_{\text{AI-IRW}}^{\text{MC}}(y, P) \right| + \left| D_{\text{AI-IRW}}^{\text{MC}}(y, P) - D_{\text{AI-IRW}}(y, P) \right| \\ &\quad + \left| D_{\text{AI-IRW}}(x, P) - D_{\text{AI-IRW}}(y, P) \right| \\ &\leq 2L_p \|x - y\| + \left| D_{\text{AI-IRW}}^{\text{MC}}(y, P) - D_{\text{AI-IRW}}(y, P) \right|. \end{aligned} \quad (20)$$

Now let $\zeta > 0$ and $y_1, \dots, y_{\mathcal{N}(\zeta, \mathcal{B}_r, \|\cdot\|_2)}$ be a ζ -coverage of \mathcal{B}_r with respect to $\|\cdot\|_2$. We know that

$$\log(\mathcal{N}(\zeta, \mathcal{B}_r, \|\cdot\|_2)) \leq d \log(3r/\zeta). \quad (21)$$

Define $\mathcal{N} = \mathcal{N}(\zeta, \mathcal{B}_r, \|\cdot\|_2)$ for notation simplicity. There exists $\ell \leq \mathcal{N}$ such that $\|x - y_\ell\|_2 \leq \zeta$. Thus, Eq. (20) leads to

$$\left| D_{\text{AI-IRW}}^{\text{MC}}(x, P) - D_{\text{AI-IRW}}(x, P) \right| \leq 2L_p \zeta + \left| D_{\text{AI-IRW}}^{\text{MC}}(y, P) - D_{\text{AI-IRW}}(y, P) \right|.$$

Applying (19) to every x_ℓ and the union bound, for any $t > 0$, it holds:

$$\mathbb{P} \left(\sup_{\ell \leq \mathcal{N}} \left| D_{\text{AI-IRW}}^{\text{MC}}(y_\ell, P) - D_{\text{AI-IRW}}(y_\ell, P) \right| > t/2 \right) \leq 2\mathcal{N} \exp(-nt^2/2).$$

yielding

$$\mathbb{P} \left(\sup_{x \in \mathcal{B}_r} \left| D_{\text{AI-IRW}}^{\text{MC}}(x, P) - D_{\text{AI-IRW}}(x, P) \right| > t/2 \right) \leq 2\mathcal{N} \exp \left(-2n(t/2 - 2L_p\zeta)^2 \right).$$

Using Equation (18), the union bound and (21), one gets:

$$\begin{aligned} \mathbb{P} \left(\sup_{x \in \mathcal{B}_r} \left| \hat{D}_{\text{AI-IRW}}^{\text{MC}}(x) - D_{\text{AI-IRW}}(x, P) \right| > t \right) &\leq \mathbb{P} \left(\sup_{x \in \mathcal{B}_r} \left| \hat{D}_{\text{AI-IRW}}(x) - D_{\text{AI-IRW}}(x, P) \right| > t/2 \right) \\ &\quad + \mathbb{P} \left(\sup_{x \in \mathcal{B}_r} \left| D_{\text{AI-IRW}}^{\text{MC}}(x, P) - D_{\text{AI-IRW}}(x, P) \right| > t/2 \right) \\ &\leq 6.9^d \exp \left(-\frac{n}{2} \min \left\{ (\kappa t/2)^2, \kappa t/2 \right\} \right) \\ &\quad + \frac{6(2n)^{d+1}}{(d+1)!} \exp(-nt^2/128) \\ &\quad + 2 \left(\frac{3r}{\zeta} \right)^d \exp \left(-2n(t/2 - 2L_p\zeta)^2 \right). \end{aligned}$$

Choosing $\zeta \sim m^{-1}$ leads to the desired result.

B.3 Geometric Results on the Lipschitz Constants in Assumptions 2 and 3

Lemma 6. *Let $r > 0$ and denote by $V_{d,r}$ the volume of the d -ball $\mathcal{B}(0, r)$. Assume that X takes its values in $\mathcal{B}(0, r)$ and has an M -bounded density w.r.t. the Lebesgue measure λ . Thus X is uniformly RADially LIPSCHITZ CONTINUOUS with constant $L_R = MV_{d,r}$.*

Proof. Let $x \in \mathbb{R}^d$. By $\|\cdot\|_g$ it means the geodesic norm on the unit sphere of \mathbb{R}^d . It holds:

$$\begin{aligned} |\phi(u, x) - \phi(v, x)| &\leq \mathbb{P} \{ X \in \mathcal{B}(0, r) : \langle u, X - x \rangle \text{ and } \langle v, X - x \rangle \text{ are of opposite sign} \} \\ &\leq M \lambda \{ z \in \mathcal{B}(-x, r) : \langle u, z \rangle \text{ and } \langle v, z \rangle \text{ are of opposite sign} \} \\ &\stackrel{(i)}{\leq} M V_{d,r} \times \frac{2}{\pi} \arccos(\langle u, v \rangle) \\ &= M V_{d,r} \times \frac{2}{\pi} \|u - v\|_g \\ &\leq M V_{d,r} \|u - v\|. \end{aligned}$$

Where (i) comes from the fact that the volume of $\mathcal{E}_{u,v} = \{z \in \mathcal{B}(-x, r) : \langle u, z \rangle \text{ and } \langle v, z \rangle \text{ are of opposite sign}\}$ is the volume of two cones of angle $\|u - v\|_g$ as depicted in Figure 3. \square

Lemma 7. *Let $r > 0$ and assume that X takes its values in $\mathcal{B}(0, r)$ and has M -bounded density w.r.t. the Lebesgue measure λ . Thus X is uniformly LIPSCHITZ CONTINUOUS IN PROJECTION with constant $L_p = MV_{d-1,r}$.*

Proof. Let $u \in \mathbb{S}^{d-1}$. By $\|\cdot\|_g$ it means the geodesic norm on the unit sphere of \mathbb{R}^d . It holds:

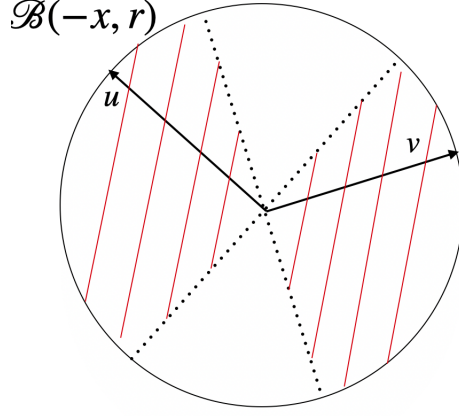


Figure 3: Illustration of the set $\mathcal{E}_{u,x,y}$ in \mathbb{R}^2 . It corresponds to the portion of $\mathcal{B}(-x, r)$ hatched in red.

$$\begin{aligned}
|\phi(u, x) - \phi(u, y)| &\leq \mathbb{P}\{X \in \mathcal{B}(0, r) : \langle u, X - x \rangle \text{ and } \langle u, X - y \rangle \text{ are of opposite sign}\} \\
&\leq M \lambda \{z \in \mathcal{B}(0, r) : \langle u, z - x \rangle \text{ and } \langle u, z - y \rangle \text{ are of opposite sign}\} \\
&\stackrel{(i)}{\leq} M V_{d-1,r} \times |\langle u, x \rangle - \langle u, y \rangle| \\
&\leq M V_{d-1,r} \|x - y\|.
\end{aligned}$$

Where (i) comes from the fact that we encompass $\mathcal{F}_{u,x,y}$ by an hyper-cylinder of length $|\langle u, x \rangle - \langle u, y \rangle|$ with $\mathcal{F}_{u,x,y} = \{z \in \mathcal{B}(0, r) : \langle u, z - x \rangle \text{ and } \langle u, z - y \rangle \text{ are of opposite sign}\}$, as illustrated in Figure 4. \square

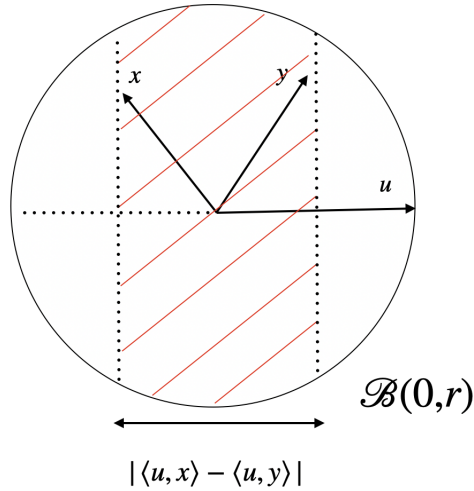


Figure 4: Illustration of the set $\mathcal{F}_{u,x,y}$ in \mathbb{R}^2 . It corresponds to the portion of $\mathcal{B}(0, r)$ hatched in red.

C Approximation Algorithm

Her, we detail the approximation algorithm of the AI-IRW depth (see Algorithm 1).

Algorithm 1 Approximation of the AI-IRW depth

Initialization: The number of projections m .

- 1: Construct $\mathbf{U} \in \mathbb{R}^{d \times m}$ by sampling uniformly m vectors U_1, \dots, U_m in \mathbb{S}^{d-1}
 - 2: Compute $\hat{\Sigma}$ using any estimator
 - 3: Perform Cholesky or SVD on $\hat{\Sigma}$ to obtain $\hat{\Sigma}^{-1/2}$
 - 4: Compute $\mathbf{V} = \hat{\Sigma}^{-1/2} \mathbf{U} / \|\hat{\Sigma}^{-1/2} \mathbf{U}\|$
 - 5: Compute $\mathbf{M} = \mathbf{XV}$
 - 6: Compute the rank value $\sigma(i, k)$, the rank of index i in $\mathbf{M}_{:,k}$ for every $i \leq n$ and $k \leq m$
 - 7: Set $D_i = \frac{1}{m} \sum_{k=1}^m \sigma(i, k)$ for every $i \leq n$
- Output:** D
-

D Additional Experiments

D.1 Illustration of Affine-Invariance

The Figure 5 illustrates the non affine-invariance of the IRW and the affine-invariance of the AI-IRW.

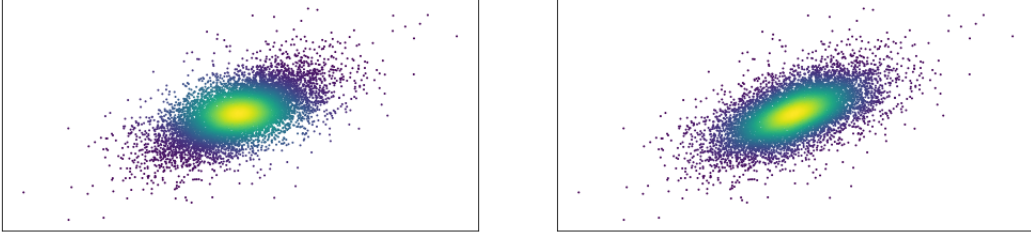


Figure 5: The IRW depth (left) and the AI-IRW (right) depth on a Student-10 distribution. The darker the point, the lower the depth.

D.2 Variance through Noisy Directions

The first experiment in Section 5 is repeated with different level of gaussian noise that are added to sampled directions, *i.e.* $U = \frac{W + \varepsilon \mathcal{N}(\mathbf{0}, \mathbf{I}_d)}{\|W + \varepsilon \mathcal{N}(\mathbf{0}, \mathbf{I}_d)\|}$. This experiment is conducted with AI-IRW, IRW, HM and halfspace depth using $m = 100$ sampled directions. The variance (over 100 repetitions) between the returned score and the original score (without noise) are computed for x_1, x_2, x_3 (same as those in the Section 5), see Figure 6. Results show that AI-IRW shares very few differences with IRW while the superiority of AI-IRW (and IRW) over the existing methods depth such as halfspace and halfspace mass is highlighted.

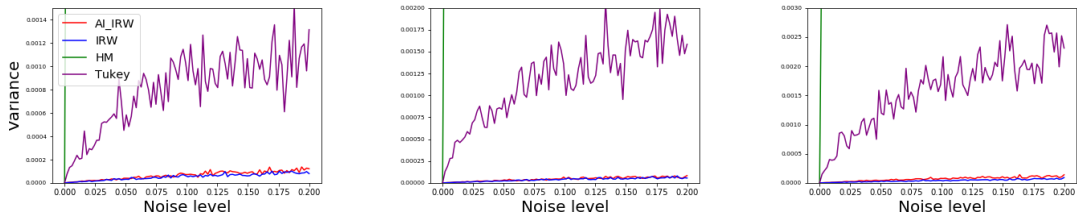


Figure 6: Variance of the score of x_1, x_2, x_3 (from left to right) over the noise level induced in sampled directions with 1000 repetitions for the AI-IRW, IRW, Tukey depth.

D.3 Anomaly Detection: a Comparison on a Toy Data Set

In this part, a comparison between AI-IRW, IRW and the halfspace depth is provided. To conduct this experiment, we construct a toy contaminated data set (see Figure 7, left) where aggregated outliers (green points) and some independant outliers (red points) are added to 1000 points stemming from a 2-dimensional *Gaussian* distribution. The 100 lowest scores are depicted (see Figure 7, right) for the three benchmarked data depths. Results show that AI-IRW is able to assign the lowest depth to these anomalies while IRW and Tukey both fail to identify them.

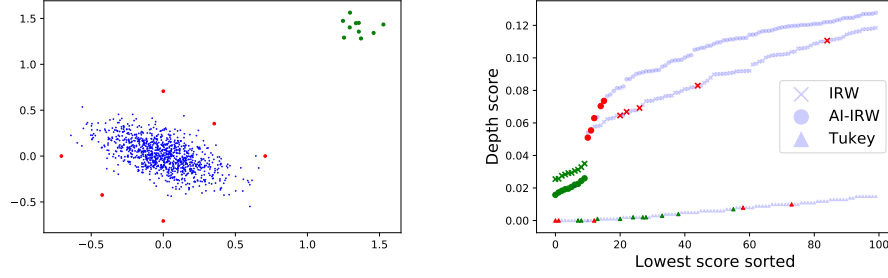


Figure 7: Toy dataset with outliers (left) and the AI-IRW, IRW and Tukey sorted scores (right).